Fluctuations, line tensions, and correlation times of nanoscale islands on surfaces

F. Szalma,[1,2,*] Hailu Gebremariam,[1] and T. L. Einstein[1,†]

[1]*Department of Physics, University of Maryland, College Park, Maryland 20742-4111, USA*
[2]*Institute of Theoretical Physics, Szeged University, H-6720 Szeged, Hungary*
(Received 23 December 2003; revised manuscript received 30 June 2004; published 28 January 2005)

We analyze in detail the fluctuations and correlations of the (spatial) Fourier modes of nanoscale single-layer islands on (111) fcc crystal surfaces. We analytically show that the Fourier modes of the fluctuations couple due to the anisotropy of the crystal, changing the power spectrum of the fluctuations, and that the actual eigenmodes of the fluctuations are the appropriate linear combinations of the Fourier modes. Using kinetic Monte Carlo simulations with bond-counting parameters that best match realistic energy barriers for hopping rates, we deduce absolute line tensions as a function of azimuthal orientation from the analyses of the fluctuation of each individual mode. The autocorrelation functions of these modes give the scaling of the correlation times with wavelength, providing us with the rate-limiting kinetics driving the fluctuations, here step-edge diffusion. The results for the energetic parameters are in reasonable agreement with available experimental data for Pb(111) surfaces, and we compare the correlation times of island-edge fluctuations to relaxation times of quenched Pb crystallites.

I. INTRODUCTION

Nanoscale islands consisting of $10^2 - 10^5$ atoms have captured great interest over recent years for a variety of reasons. From a practical standpoint, they provide a precursor to the formation of quantum dots, which, if assembled in a controlled way, can serve as the basic ingredients of nanoscale electronic and mechanical devices. Many crystallites or nanomounds are best viewed as "wedding-cake"-like stacks of such islands.[1] They are the intermediary between a flat surface and a small three-dimensional structure. In contrast to steps, which require vicinal surfaces[2] that often must be well characterized over mesoscopic regions, islands can be studied in smaller-scale regions that are flat only locally.

Of particular interest to us are the shape and the fluctuations of the perimeter of these islands. The shape provides information about the line tension or step free energy per length, from which one can compute the step stiffness that describes the "inertial" properties of steps. The "dipole" mode of these fluctuations are known to underlie the diffusion of such islands, a concept now used routinely in simulations.[3,4] However, shorter-wavelength modes are also of great interest, since they can be correlated with similar fluctuations of steps and provide a way to assess, again, the stiffness of the step and also the kinetic or atomistic diffusion coefficient associated with the mechanism that dominates the atomistic processes underlying the fluctuations. Until recently, attention was limited to structures for which crystal anisotropy could seemingly be ignored.

Here we pay particular attention to the role of the inevitable anisotropy of crystal surfaces, which around room temperature or even above it is typically sufficiently strong that it should apparently be taken into account in order to correctly characterize the morphology of the various (near) equilibrium structures appearing on surfaces and their dynamics. In this paper we focus on the line tension and stiffness and their orientation dependence; we give an analytic method to calculating these physical parameters from the fluctuation of nanoscale islands.

The little experimental data on such systems involve runs of worrisome duration or use probes that provide scanned rather than instantaneous images. To generate fullycharacterized data, we turned to kinetic Monte Carlo (KMC) simulations to mimic the equilibrium fluctuations of islands. These simulations are the input of our analytic theory which, starting from the excess free energy corresponding to the capillary wave fluctuations of the island edge, provides the eigenmodes of these fluctuations. Since the two-dimensional (2D) Wulff plot relating the equilibrium island shape and the line tension in the azimuthal directions on the surface provides only relative line tensions for various orientations, a key problem is always the determination of the chemical potential λ of the island edge, which then produces an absolute relation. This potential can be determined with surprisingly good ($\sim 10\%$) accuracy from the spectrum of the modes of the system. We compare these eigenmodes and the simple Fourier modes of the fluctuations and reach the (perhaps) surprising conclusion that the anisotropy only affects the longer wavelength modes.

Another aim of the paper is to examine the correlation of the fluctuations of the Fourier modes and thereby to find the rate-limiting process driving the fluctuations in a fairly realistic model. For our KMC simulations we sought a system for which one could compute hop rates with good accuracy and for which there was quantitative experimental data with which to compare. Accordingly, we have chosen Pb(111) so as to be able to compare with intriguing recent experiments by Thürmer *et al.*.[5] This analysis gives the scaling of the correlation time with the wavelength, that is the dynamic exponent z, and provides us with characteristic times measured not only in MC steps, but in real time. Thus, we can compare directly with experiments and extrapolate to different structures from the simple one considered here. (See Fig. 1.)

Utilizing direct surface imaging techniques, especially scanning tunneling microscopy (STM), several attempts have
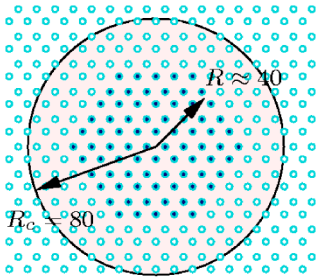
FIG. 1. (Color online) Geometry of the MC simulation. The approximate mean radius R of the island and the radius R_c of the container are illustrated.

been made to measure and calculate step energies. From a theoretical viewpoint the various methods that used the experimental data for calculations can be broken down into two main groups. The first is based on a lattice model which relates the island shape (radius and curvature) to the temperature dependence of the free energy and stiffness of the Ising model in the low-temperature expansion, usually in high symmetry directions. By fitting the functional shape of the free energy with varying temperature on the experimental data determined by the equilibrium island shape[6] gives the Ising kink energy, which in turn provides the step energies and stiffnesses. However, limitations of the Ising model to describe surface structure have recently been noted.[7]

The other method is based on a step continuum model which makes use of stochastic differential equations to describe the fluctuations of straight steps[8] or island edges[9,10] viewed as nearly circular closed-loop steps. Thus, the initial calculations for island fluctuations assumed isotropy,[11] the power spectrum of the Fourier modes of the step fluctuations were calculated and adapted with appropriate modifications to nearly circular island shapes.[12] If the anisotropy turns out to be strong, it cannot be handled as a perturbation; a complete anisotropic calculation without any such assumptions becomes necessary.

This challenge was recently taken up by Khare *et al.*,[13] who give an approximate form for the free energy functional and calculate the chemical potential integrating all the Fourier modes in the system by using the generalized equipartition theorem where the modes are buried in a sum. However, these modes are coupled, so any one mode missing (e.g., due to lack of experimental resolution) in the sum can contribute to a deviation from the precise value of the chemical potential by itself and through its coupling to the other modes as well. In contrast, our approach of analyzing individual modes gives more insight into the extent to which this coupling should be taken into account, and provides the chemical potential in a (mathematically) controlled way.

The autocorrelation function of fluctuations of step edges and correlation times have been analyzed theoretically in Fourier space based on the Langevin formalism,[11,14] and experimentally in the context of straight-step fluctuations on Si(111) (Ref. 15) and Si(001) (Ref. 8) surfaces for relatively long wavelengths. The rate-limiting kinetics driving these fluctuations are determined by the dynamic exponent, which also sets the universality class to which the system belongs.[16]

(The roughness exponent is believed to be $1/2$ in our cases.) The correlation times are theoretically identical to the relaxation times (or, in some cases, decay times) of surface features,[17,18] such as decay and near-equilibrium build-up of bulges (of either sign) along the step edge that also have (wave)length L. Three-dimensional features like mesoscopic (or smaller) wires on surfaces as well as the surface corrugations in earlier studies by Mullins,[19,20] are typically described by $1+1$ dimensional models but may involve different, more complicated mechanisms driving their fluctuation or decay. We will compare and discuss these various relaxation times in the paper.

The paper is organized as follows: In the next section we give an analytic solution to the decoupling of the Fourier modes of the system into the actual eigenmodes and recalculate the free energy functional of the edge fluctuations. The results and conclusions can be understood without the reader going through this algebra; only the result expressed in Eq. (10) is used later. In Sec. III we introduce the KMC simulation and in Sec. IV use the results to calculate the chemical potential and line tension. In Sec. V we calculate the correlation functions of the Fourier modes and deduce the scaling of the correlation time with length, the dynamic exponent z. We compare with available experimental data for Pb(111). Section VI concludes the paper.

II. FOURIER MODES, EIGENMODES

The relationship between the equilibrium crystal shape and the surface tension or, in our 2D case, between the equilibrium island shape and the line tension of its edge can be established by the minimization of the free energy functional of the island edge. The orientation-dependent line tension $\beta(\mathbf{n})$ is defined as the work per unit length necessary to create the ds line element with normal $\mathbf{n}$ to the perimeter. The free energy is the integral of this work along the whole perimeter. The equilibrium island shape at a constant temperature T, number of particles N, and area Σ, is determined by the minimization of the free energy functional with respect to the shape with the constraint that the island area is constant, typically using the method of Lagrange multipliers,[21]

$$F[R, \dot{R}, \theta] = \oint_{L_{eq}} \beta(\mathbf{n})ds - \lambda \int_{\Sigma} d\sigma$$
$$= \int_0^{2\pi} \beta(\psi(\theta))(R^2 + \dot{R}^2)^{1/2}d\theta - \lambda \int_0^{2\pi} \frac{R^2}{2}d\theta.$$
$$(1)$$

Here the second line is in polar coordinates with θ the polar angle and $R(\theta)$ the radius of the equilibrium shape. The dot denotes the differentiation with respect to the angle, λ is the Lagrange multiplier (which actually turns out to be the chemical potential), and ψ is the angle which characterizes the vector normal to the shape (see Fig. 2). ds and $d\sigma$ are the line element and surface element, respectively. Formally minimizing the $F = F[R, \dot{R}, \theta]$ functional, the Euler-Lagrange equation gives a relation between the equilibrium island
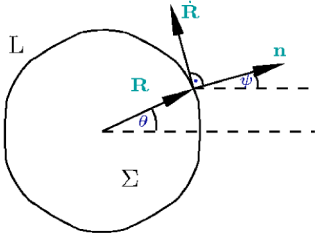
FIG. 2. (Color online) Schematic showing variables used to analyze equilibrium island shape
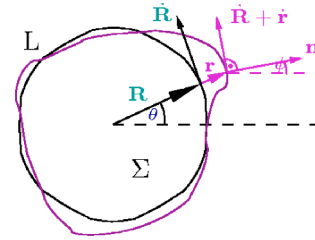

FIG. 3. (Color online) Extension of Fig. 2, showing instantaneous island shape, for analysis of fluctuations. For a particular azimuthal direction, θ, the deviation from the equilibrium island shape, r, its derivative with respect to θ, $\dot{r}$, the unit vector normal to the instantaneous shape, $\mathbf{n}$, and the corresponding angle, ψ, are all time dependent.

shape $R(\theta)$ and the orientation dependent line tension, $\beta(\psi)$, and between the two angles involved, ψ which depends on the polar angle and the equilibrium shape,[13,22]

$$\frac{\delta F}{\delta R} = 0 \Rightarrow \begin{aligned} \beta(\psi) &= \lambda \frac{R^2}{(R^2 + \dot{R}^2)^{1/2}} \\ \psi &= \theta - \arctan \frac{\dot{R}}{R} \end{aligned}. \quad (2)$$

However, in this procedure λ is a prefactor and cannot be determined, leaving the relation relative. Equation (2) is the seminal Wulff construction in polar coordinates.

In order to determine the chemical potential, the thermal fluctuations of the island edge can be utilized. In this case the free energy of the island changes as its shape changes due to the fluctuations, and the free energy is certainly not at its minimum but depends on the island's instantaneous shape. Then the free energy of this instantaneous shape is the integral over the line elements of the shape with their corresponding line tension, which changes with time as the orientation of the shape element changes,

$$F[r, \dot{r}, \theta; t] = \oint_L \beta(\mathbf{n}) ds$$
$$= \int_0^{2\pi} \beta(\psi(\theta))((R + r)^2 + (\dot{R} + \dot{r})^2)^{1/2} d\theta. \quad (3)$$

Here r and $\dot{r}$ are time dependent and describe the deviation of the instantaneous shape from the equilibrium one as shown in Fig. 3. The angle ψ is also time dependent since now it depends not only on R and $\dot{R}$ as in Eq. (2), but also on r and $\dot{r}$. Considering only small deformations from the equilibrium shape (as it is usually assumed in the capillary wave theory) and also small slope deviations from the equilibrium slope $\dot{R}$, so that $r, \dot{r} \ll R$, the Taylor expansion (both in β and in the square root) in these small parameters leads to the functional

$$F[r, \dot{r}, \theta; t] = \lambda \int_0^{2\pi} \frac{1}{2} \frac{(\dot{R}r - R\dot{r})^2}{R^2 + 2\dot{R}^2 - R\ddot{R}} d\theta. \quad (4)$$

This functional contains three quadratic terms $A(\theta)r^2$, $Q(\theta)r\dot{r}$, and $B(\theta)\dot{r}^2$. The cross term Q drops out after taking the ensemble average; both the two other terms are determined by properties of the equilibrium island shape,

$$A(\theta) = \frac{1}{2} \frac{\dot{R}^2}{R^2 + 2\dot{R}^2 - R\ddot{R}}, \quad (5)$$

$$B(\theta) = \frac{1}{2} \frac{R^2}{R^2 + 2\dot{R}^2 - R\ddot{R}}, \quad (6)$$

and provide the weightings of the fluctuations of the deformations characterized by r^2 and $\dot{r}^2$, respectively. These deformations at the microscopic level are due to the thermal movement of adatoms surrounding the island constantly attaching to its edge and coming off from it.

To diagonalize the free energy one rewrites the integrand in Fourier form,

$$F[\{r_n\}; t] = 2\pi\lambda \sum_{m,n} (A_{m-n} + mnB_{m-n}) r_n(t) r_m^*(t), \quad (7)$$

where $r_k = \int_0^{2\pi} r(\theta) \exp[ik\theta] d\theta$ and similarly for A_k and B_k. The Fourier modes are coupled due to the anisotropy, which is contained in A and B as we shall see shortly. Here $n=0$ is the expansion-contraction mode; $n=1$, which we called the dipole mode in the Introduction, is related to the Brownian, diffusive motion of the island; $n=2$ is a quadrupolar distortion, i.e., an elongated shape with two maxima and two minima in perpendicular directions, and so on. The Fourier components have Hermitian properties since $A(\theta)$ and $B(\theta)$, the factors associated with the equilibrium island shape, are real functions; hence, $A_{-i} = A_i^*$, $B_{-i} = B_i^*$, and $r_{-i} = r_i^*$.

The free energy of Eq. (7) can readily be cast into matrix form,

$$F[\mathbf{r}; t] = 2\pi\lambda \mathbf{r}^\dagger (\mathbf{A} + \mathbf{MBN}) \mathbf{r}, \quad (8)$$

where $\mathbf{r}$ is a vector containing the Fourier components of the instantaneous island shape, $\mathbf{A}$ and $\mathbf{B}$ are Hermitian matrices, $[\mathbf{A}]_{m,n} = A_{m-n}$, $[\mathbf{B}]_{m,n} = B_{m-n}$, and $\mathbf{M} = \mathbf{N}$ are diagonal matrices with the wave numbers along the diagonal.

As in practice there are only a finite number of atoms on the edge of the island, we discretize the problem. If the number of atoms on the edge is $2N$, there are as many modes in the system; as we will see in Sec. IV, to analyze the right number of modes is crucial to the problem. Now, if $\mathbf{r}$ contains the r_k Fourier components from $-N+1$

through N, the Fourier transform is discrete and $r_k = \Sigma_{j=-N+1}^{N} r_j^\theta \exp[i \, k \, j\pi/N]$, where r_j^θ is the deviation from the equilibrium shape in the $\theta = j\pi/N$ direction.

The A_k and the B_k can be obtained similarly, and **A** and **B** are finite cyclic Hermitian matrices, meaning that their diagonal elements are the same. They also reflect the symmetry of the equilibrium shape as, e.g., in our case due to the six-fold symmetry the principal diagonal is filled with A_0, the sixth to the right with A_{-6}, etc. As **M** and **N** are the same diagonal matrices, the **MBN** product keeps the Hermitian property.

In the isotropic case (when the equilibrium shape is circular), $A(\theta)=0$ and $B(\theta)=1/2$ for all θ. After the Fourier transformation this gives **A**$=0$ (zero matrix) and **B**$=(1/2)\mathbb{1}$ (diagonal matrix). The anisotropy comes into play when the equilibrium shape is not circular, so that $A(\theta)$ and $B(\theta)$ are not constants and their higher order Fourier components fill the (off-)diagonals. These off-diagonals couple the Fourier modes.

Due to Hermiticity the above matrix form is diagonalizable,

$$F[\{h_n\};t] = 2\pi\lambda \sum_n \Lambda_n h_n h_n^*, \qquad (9)$$

and the eigenvalues Λ_n of the **A**$+$**MBN** matrix are all real. As we see below [in Eq. (10)] these eigenvalues are related to the strengths of the h_n eigenmodes, which at every time instant are just the transforms of the $r_n(t)$ Fourier modes of the instantaneous island shape. Again due to Hermiticity, there is a unitary matrix **U** which transforms Eq. (8) into Eq. (9) and gives the linear relationship between **r** and **h**, **r**$=$**Uh**, where the vector **h** contains the h_n as its elements.

This decomposition of the free energy into eigenmodes in Eq. (9) facilitates the calculation of the Lagrange multiplier λ. In equilibrium, according to the equipartition theorem, the ensemble average of each mode, representing a degree of freedom, must have the same Boltzmann energy,

$$2\pi\lambda \overbrace{\Lambda_n \langle |h_n|^2 \rangle}^{E_n} = \tfrac{1}{2}k_B T. \qquad (10)$$

Λ_n and can be determined from the equilibrium island shape and the fluctuating island perimeter, respectively. Here E_n must be a constant in n, the modes, as the temperature and the chemical potential, λ, are fixed macroscopic parameters of the island. From this equation one can determine the same λ, in principle, from any mode. Thus, either experimentally observing island fluctuations or using Monte Carlo simulations one can determine E_n, which in turn provides λ. This λ was the missing parameter to determine absolute line tensions, and plugging it back into Eq. (2), we get the line tension in all azimuthal directions.

III. KINETIC MONTE CARLO

The scarcity of extensive experimental data leads us to use Monte Carlo methods to simulate the behavior of the system. However, use of numerical rather than experimental data for testing of formal ideas has many advantages in any case. Most obviously, in numerical experiments one can obtain far greater control, with no worries about anomalous behavior due to unsuspected stray contaminants. Typically one can generate much more data. In the present experiment, we do not need to worry about the scan rate of the probe; our lattice configurations are instantaneous snapshots. Another advantage of computer simulations will also become clear in the next section: it allows us to analyze correlation times.

Since our original motivation was to simulate the relaxation of a Pb crystallite with a (111) facet, we place a nanoscale island on a triangular lattice. We surround it by a nonpermeable circular container of radius R_c to let the system reach its thermodynamic equilibrium, in order to measure its equilibrium fluctuations.[23,24] Thus, this geometry corresponds to an island placed on top of a facet of a crystallite (with an infinite Ehrlich-Schwoebel barrier). Note that by adjusting the permeability one can tune the overall decay rate of the island, which in this paper we fix at zero.

Since the temperature of the systems of interest is low compared to the energy barriers of adatomic hopping, we have chosen to use the Bortz-Kalos-Lebovitz (BKL) continuous-time MC algorithm[25] as it is best suited to low temperature systems and as its rejection-free method allows us to greatly improve the efficiency of the simulations compared to traditional Metropolis algorithms. The typical temperatures are around $T_c/4$ or less for the two-dimensional lattice gas of adatoms on the surface. Using the n-fold way method to keep track of the available MC moves, we could improve the efficiency even further. Because of the small number of energy barriers, the n-fold way approach (five-fold) is superior to the binary tree implementation of the BKL algorithm[26] in this case.

Since we are not interested in all the details of this surface in the simulations, but only try to capture the main mechanisms, we do not take into account the *ABC* stacking structure of the fcc lattice of Pb(111). Hence, the top layer constitutes a triangular lattice with perfect sixfold symmetry. Furthermore, we assume that adatoms can only hop to nearest-neighbor sites, and that the energy barrier the adatom must overcome is determined by the occupation of the eight sites surrounding, as nearest neighbors, the two sites involved in the hopping process.

The energy barriers for hopping rates are mainly based on the semiempirical embedded atom method (SEAM)[27] using Ercolessi's glue potentials[28] for the Pb(111) surface to derive the bond-counting energy barriers[26] actually used in the simulations (see Table I). We use variants of simple bond counting. In what we term the break-three scheme, we count only bonds that have been broken with the three sites "behind" the move. If we also include bond breaking with the two sites to the left and the right of the move (denoted side sites), we have a break-five scheme. The three sites in front of the move do not affect the energy barrier in our simulations. The break-three and break-five schemes both satisfy detailed balance in a straightforward fashion. They both should give the same results for static parameters, since they are both nearest-neighbor schemes. Comparison runs using this feature provided one test (among many) of our program. However, the kinetics obviously differ because the energy barriers tend to be higher for the break-five scheme, slowing

TABLE I. Tabulation of some of the energy barriers used in KMC simulations of Pb(111). The energies in columns 2 and 3 were computed by Haftel using SEAM (Ref. 27) with glue potentials (Ref. 28). In the last column are the energies used in the simulations. [The edge-diffusion energy barrier in the break-three scheme is closer to the corner rounding barrier of SEAM than to the actual straight-edge diffusion barrier of SEAM (see text); the latter has a much lower barrier: 108 meV; unfortunately, the bond-counting method does not distinguish between these two.]

Process	Energy (meV)	Energy (K)	Break-three energy (K)
Surface diffusion	70	812	812
Edge diffusion	237	2749	2319
Break 1 bond	192	2227	2319
Break 2 bonds	359	4164	3826
Break 3 bonds	467	5417	5333
Attachment			812
Out			70000

the kinetics significantly. Since the energy barriers in the break-three case are closer to the calculated barriers, we choose to use this scheme in our simulations.

In Table I we list a few energy barriers calculated by the above-mentioned SEAM and the corresponding break-three-scheme barriers. Surface diffusion is when an adatom has no other adatoms in the surrounding eight sites in SEAM calculations; in the break-three scheme this barrier also applies to all cases in which any of the side sites or the sites in front are occupied. This is the reason why the attachment barrier is the same as the surface diffusion barrier. Edge diffusion is the case in which a side site is occupied, as is its nearest neighbor "behind." The energy barrier associated with this process is 237 meV whereas if there is a nearest in the front as well so that the adatom rolls along three others on one side the third in the front seems to assist the hop a great deal (at least according to the SEAM data) as the barrier is 108 meV. The break-three scheme has the same barrier for these two processes and also for any other in which only one bond is broken. The break-two-bonds barrier corresponds to a hop with two occupied sites in the back, break-three bonds is when all three sites are occupied in the back. The very high "out" energy barrier assures that adatoms cannot escape the container; i.e., the permeability is zero.

The basic parameters of the surface investigated and the KMC simulations are the following: The nearest-neighbor spacing a_1 on the Pb(111) surface is 3.50 Å. The typical island diameter $2R$ is $40a_1$ to $80a_1$, while the container diameter R_c ranges from 12.5% to 300% larger than the island. We examined temperatures 250 K, 300 K, 350 K, and 400 K. In each MC snapshot of the island, we measure the island radius from the instantaneous center of mass in N "equiangular" directions where $N=360$ if not indicated otherwise.

We start the simulations from a nearly circular shaped configuration and let it relax to equilibrium, starting the MC measurement of the fluctuation and shape after the longest wavelength mode has passed its correlation time. Especially at the lower temperatures, the typical equilibration times are
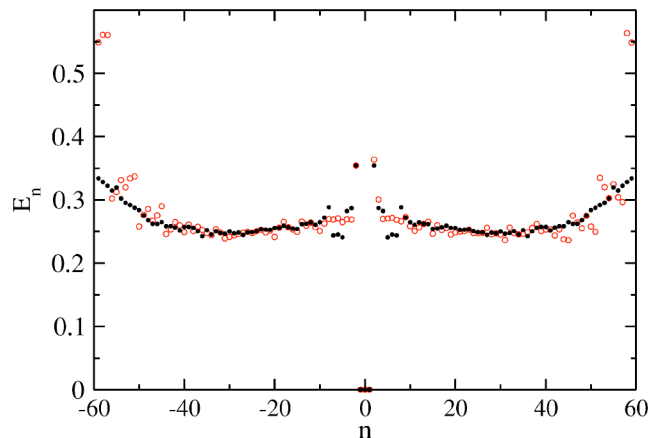

FIG. 4. (Color online) Eigenmodes (open squares) and Fourier modes (solid circles) at $T=250$ K, $R=20a_1$, $R_c=40a_1$. E_n is measured in atomic spacing units.

very long, consistent with other reports.[29,30] Ensemble averages are taken from 100 to 3000 different runs starting from the same initial configuration, but with different random-number seeds. In each run, after equilibration, we get statistically independent fluctuations at time intervals again determined by the relaxation time of the longest wavelength mode. We take such independent "snapshots" of the islands 5 to 200 times in each run, so that we typically have 10 000 to 70 000 islands over which to average.

IV. CHEMICAL POTENTIAL, LINE TENSION, LINE STIFFNESS

As described in detail in Sec. II, the energetic parameters of the island edge are determined by the island shape and its edge fluctuation. The Wulff construction provides the relationship between the relative line tension in the azimuthal directions on the crystal surface and the equilibrium island shape, and the information from the fluctuations $\langle |h_n|^2 \rangle$ of each mode in Eq. (10) gives the chemical potential λ that makes the Wulff construction absolute in Eq. (2).

From our KMC simulations we determine E_n of Eq. (10); it is depicted in Fig. 4 for $T=250$ K and $R=20a_1$ island radius. Since the perimeter is about $120a_1$, we use 120 points to describe the circumference out of the 360 available.

We calculate E_n both using the transformation to the eigenmodes taking into account the anisotropy, and also pretending the islands were isotropic. In this latter case the $h_n=r_n$ are simply the Fourier modes, and $\Lambda_n=(1/2)n^2$.

The Fourier modes and the eigenmodes are nearly indistinguishable (cf. Fig. 4) except for long wavelengths (small wave number n). The "fluctuations" in the Fourier modes for longer wavelengths are the only signature of the anisotropy. This effect is smoothed out by transforming to the eigenmodes. (Only the longest [$n=2$] wavelength mode seems to stand out after the transformation. We are still puzzled that the longest wavelength is so special and does not couple to the shorter wavelength modes. We give a more detailed account of the analysis of the coupling elsewhere.[40]) The

chemical potential can be determined from either the Fourier modes or the eigenmodes using their plateau regions (between $n=4$ and $n=40$); however, since only the longest-wavelength modes (if any) are measurable due to the poor temporal resolution of present-day experimental apparatus (see the results for correlation times in the next section), the transformed modes serve better for determining chemical potentials. Finding E_n thus from these intermediate wave numbers, gives $E_n=0.275a_1^2$ and through Eq. (10) and Eq. (2) $\beta=34.1$ meV/Å for the line tension for the high-symmetry direction. This value reasonably approximates the experimentally obtained ones for Pb(111) at $T=393$ K, $\beta_{1A}=27.9$ meV/Å and $\beta_{1B}=26.5$ meV/Å for A- and B-type steps, respectively, considering the crude approximation of bond-counting mentioned earlier.[31] In our simulations the two directions corresponding to the two different types of steps are intrinsically equivalent because we assume sixfold symmetry as the available values for energy barriers that we use in our KMC do not distinguish between the A and B directions, as mentioned in Sec. III.

At higher temperatures the Fourier modes deviate less from the eigenmodes for longer wavelengths, as expected since the equilibrium shape is more nearly circular and less affected by the underlying anisotropy.

In earlier work[13,22] in which experimental data were used as an input of similar calculations, there is a sum over the modes, but because those modes are buried in a sum in the generalized equipartition theorem, one cannot see whether they are the modes which satisfy, at least to a certain extent, the equipartition theorem. In those experimental data the correlation times of the modes are not known and the effect of the finite temporal resolution of the experiment may also interfere with the fluctuations which should in principle be determined from "snapshots," i.e., fast scanned images—fast at least compared to the correlation times of the modes used in such calculations. We shall elaborate on this in the next section.

For the same temperature we do the same measurement as above, but monitored $N=180$ points on the perimeter instead of $N=360$. The Fourier modes are depicted in Fig. 5. There are approximately 120 atoms on the perimeter, but since we cannot divide the 180 perimeter points into 120 equiangular ones to do a Fourier transform, we use $N=90$ or $N=180$ perimeter points as an approximation and observe how the plateau changes from what we saw in Fig. 4. The comparison of these two plots from MC simulations might help analyze experimental data with limited spatial resolution as well, as it shows how the Fourier modes behave in case of undersampling ($N=90$) and oversampling ($N=180$). The undersampled modes give higher values for E_n than expected for modes $|n|>25$, as if those modes took over the energy of the modes that are missing from spectrum (namely $45<|n|\leqslant 90$). In oversampling there is not enough energy for all modes in the sampling, so they go below the expected value of E_n. This is the simple reason for the peculiar shape of the two curves in Fig. 5. The value of E_n can still be determined quite accurately by using the value at which the two curves start to separate at $|n|\simeq 10$, providing basically the same result for E_n as before.

From the equilibrium island shape using the Wulff construction, we have determined the relative line tensions and
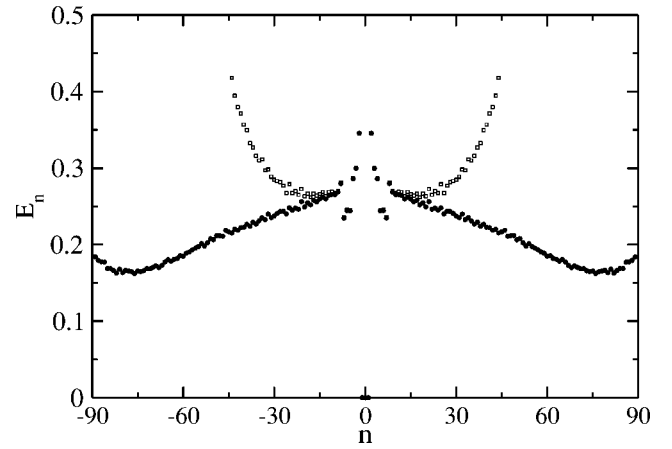

FIG. 5. Fourier modes for $N=90$ points (open squares) and $N=180$ points (solid circles) on the perimeter at $T=250$ K, and $R=20a_1$, $R_c=40a_1$. E_n is measured in atomic spacing units.

stiffnesses in the azimuthal directions on the (111) surface (see Fig. 6). The equilibrium shape is more and more "faceted" in the six main directions as we can expect, the stiffness is about 3 times bigger in the direction of the "facet" than in the direction of the corner for $T=350$ K, whereas this factor is about 20 for $T=250$ K, so that it spikes out much more, but still has only a smaller effect on the spectrum as shown before.

V. AUTOCORRELATIONS, CORRELATION TIMES, KINETICS

Inspecting the autocorrelation functions in Fourier space, we find that the longest wavelengths have surprisingly long
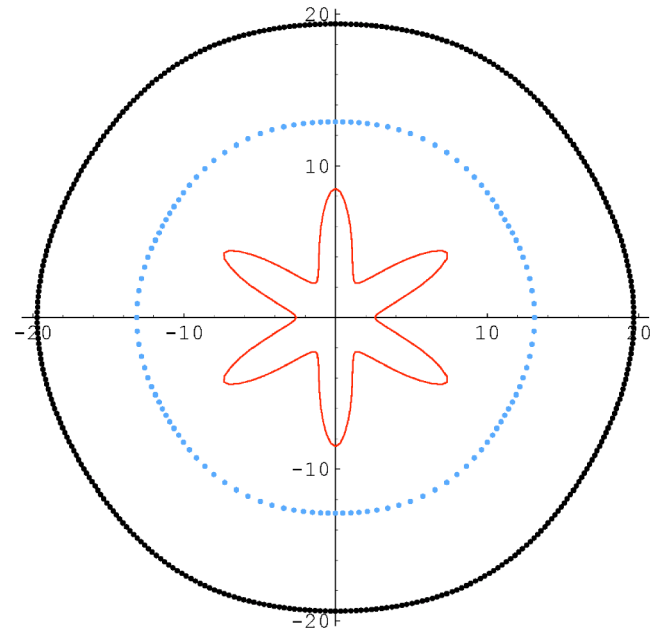

FIG. 6. (Color online) Polar plot of the equilibrium island shape $R(\theta)$ (outer dots), the relative line tension $\beta(\psi)$ (inner dots) and the relative line stiffness $\bar{\beta}(\psi)$ (the innermost curve) in arbitrary units at $T=350$ K, $R=20a_1$, $R_c=40a_1$. (Note the difference between θ and ψ.)

correlation times (in CPU time). Thus, for our fairly large (at least for the computer) systems, it is hard to reach full equilibration needed to make the desired MC measurements. Most surprising is that the relaxation time of the longest-wavelength modes is 10 to 100 times longer than the relaxation time of the islands to their equilibrium shape. Hence, estimating the thermalization time from just the shape relaxation may be very misleading, possibly giving problematic results not characteristic of equilibrium. Such behavior may include illusory strong-mode coupling, or stronger fluctuations in autocorrelation functions even in case of good statistics.

The temporal correlations can be characterized by

$$G(t) = \langle [r(t_0) - r(t_0 + t)]^2 \rangle \propto t^{2\beta}. \quad (11)$$

Since we measure correlations in equilibrium, t_0 must be greater than the thermalization time of the system. Here $r(t)$ is the fluctuation from the equilibrium shape, as before, and depends on the angle, θ, and time. The growth exponent[16] β characterizes the temporal behavior of the fluctuations. The average is taken over angles and an ensemble as well.

The typical behavior of the correlation function is that the exponent β remains at 1 for very short times,[29] typical of the ballistic behavior of diffusion at very short times, and then crosses over to a value which characterizes the rate-limiting kinetics driving the fluctuations of the island edge; eventually it crosses over to zero as the correlation function saturates due to the finite size of the system.

Pure rate-limiting kinetics have been thoroughly investigated.[11,14,32–34] In these well-defined cases, β can take the values $1/4$ for attachment-detachment kinetics, $1/6$ for surface diffusion, and $1/8$ for step-edge diffusion, where the last mechanism gives a very "slow" dynamics. There can be crossover regimes between these pure cases, leading to values of β between the quoted values, and certain geometries can also effect the value of β. One should also see crossovers as length scales vary.[11,14,34]

To investigate the length-scale dependence of the correlation function, it is more appropriate to use the correlation function in Fourier space,

$$G_n(t) = \langle |r_n(t_0) - r_n(t_0 + t)|^2 \rangle \quad (12)$$

$$= C_n(1 - \exp(-|t|/\tau_n)), \quad (13)$$

where the C_n are two times the amplitudes of the fluctuations of the modes analyzed in the preceding section, and the τ_n are their correlation times. The wave-number dependence of τ_n is known to have an intimate relationship with the exponent in $G(t)$, namely

$$\tau_n \sim n^{-z}, \quad (14)$$

where z is the dynamic exponent, and the scaling relationship between z and β here is $z = (1/2)/\beta$.[16] The correlation time increases with increasing wavelength, with the scaling exponent z. For larger exponent z, the correlation times grow more rapidly, so that for longer wavelengths the correlations and the dynamics in general can slow down very "quickly."

Here we pay particular attention to the longest wavelength and its corresponding correlation time τ_2, which makes the
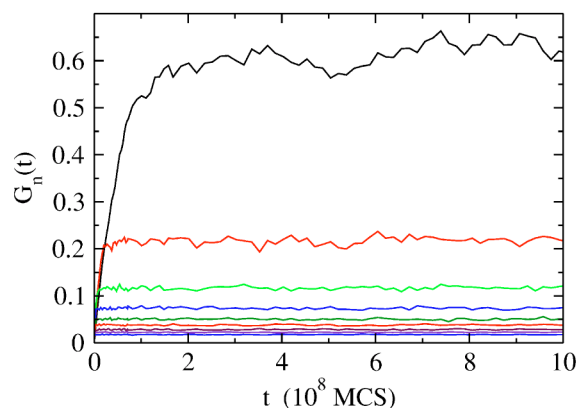

FIG. 7. (Color online) Correlation function $G_n(t)$ of the Fourier modes for $n = 2, 3, \ldots, 10$ from top to bottom. $T = 400$ K, $R = 20a_1$, $R_c = 40a_1$.

largest contribution to the fluctuations and relaxes the most slowly. From the wavelength dependence of the correlation time, we also determine the dynamic exponent and the rate limiting kinetics.

In the KMC simulations for $T = 400$ K and $R = 20a_1$, the longest-wavelength mode, $n = 2$, is $120a_1$ or 420 Å long. From Fig. 7, its relaxation time is $\tau_2 = 5.5 \times 10^7$ MCS (Monte Carlo steps). To give a crude estimate for τ_2 in real time, we consider the hopping rate

$$\nu = \nu_D \exp[-\beta E_b] \quad (15)$$

to be the product of the attempt frequency, which we identify with the Debye frequency of Pb: $\nu_D = 1.83 \times 10^{12}$ Hz,[35] and the Boltzmann factor of the energy barrier of a particular hop. Hence, a MCS in this Monte Carlo simulation is equivalent to a $1/\nu_D$ time increment in real time; thus, the relaxation time in this particular case is $\tau_2 = 0.030$ ms.

As expected, these correlation times change dramatically with temperature as the underlying physical phenomena are activated. For $R = 20a_1$ at $T = 350$ K, $\tau_2 = 2.0 \times 10^8$ MCS or 0.11 ms, which means four times longer relaxation compared to 400 K, while for 300 K $\tau_2 = 7.1 \times 10^8$ MCS or 0.39 ms, which represents slowing by another factor of 4.

We note here that we did two sets of KMC simulations. The simulations described in this paper satisfy detailed balance and sample the canonical distribution, while in the other set we choose the energy barriers to be those calculated by SEAM, which explicitly violate detailed balance and energy conservation. Interestingly, the latter simulations tend to give closer agreement with experimentally measured correlation time data. We do a comparison of the results of these two sets of simulations[40] and upcoming experimental data[41] elsewhere.

The scaling of the relaxation time with (wave)length can be seen in Fig. 8. In the plotted wave-number range, overall, τ_n basically behaves like $z = 4$, suggesting that the mechanism driving the fluctuations is step-edge diffusion which is in agreement with previous observations.[36,37]

Comparison of these length scales and their corresponding relaxation times with existing experimental observations might give interesting physical insight. For example, in the
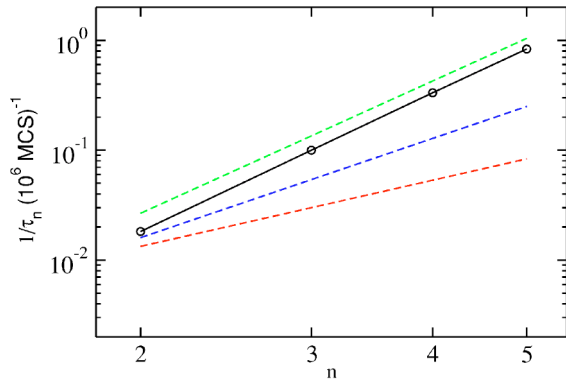
FIG. 8. (Color online) Correlation time τ_n vs wave number n on a log-log scale. The MC data (black circles) show $z=4$ which corresponds to step-edge diffusion. The dashed lines represent $z=4$, 3, and 2 (from top to bottom) dynamic exponents. $T=400$ K, $R=20a_1$, $R_c=40a_1$.

experiment by Thürmer *et al.*,[5] a small Pb crystallite, whose top facet has a perimeter slightly larger than 1200 nm, relaxes at 383 K to its equilibrium (or at least metastable) shape in 1–2 days after being quenched from a higher temperature. Since the crystallite is 30 times larger than the longest wavelengths in our KMC simulations, the relaxation time τ_{relax} of the longest wavelength mode of the perimeter of the topmost island on the crystallite is 8.1×10^5 times longer if the rate-limiting kinetics is step-edge diffusion (though, of course, attachment-detachment and terrace diffusion could be present but not rate limiting). Specifically, the value of τ_{relax} is 24.3 s based on our KMC data at $T=400$ K. From these data it seems that the island fluctuation is much faster than the decay of the three-dimensional (3D) structure; thus there is no direct relationship between the fluctuation and the decay.

The above arguments lead to a general view of the evolution of surface structures. For Pb in the temperature range 350 K–400 K, one observes the slow development and relaxation of fluctuations at the μm scale in experiments. Assuming that the rate-limiting kinetics retain the same $z=4$ range for even longer wavelengths, structures of 10 μm size—step edges, islands, etc.—take days to years to change due to the large dynamic exponent, z, so in effect they look frozen under laboratory conditions. This is the reason why these monolayer structures do not show any large-scale changes while on a shorter scale they can be very active. The structural changes in the 3D crystallites are even slower, they are even more stable.

Lowering the temperature makes the length scales—at which evolution or relaxation can be observed— exponentially shorter, which is readily understandable if one looks at the converse of the above arguments. The length scales with time like $l \sim \tau^{-1/4}$ (for $z=4$) whereas τ scales like $1/\nu$ in Eq. (15). Thus, the length scales with temperature like $l \sim \exp[E_b/4k_BT]$. This basically means that given the temperature and the time scale of observation, one can calculate an effective length scale, L_{eff} on which the structures on a surface are in equilibrium with their surroundings and actively changing on the time scale of, e.g., STM measure-

ments. Having L_{eff} and the energy barrier E_b at a certain temperature, one can also make at least rough estimates of the effective lengths at other temperatures using this scaling argument. This picture is certainly a result of simplification, since there is a whole set of energy barriers in such a complex physical system as a crystal surface, and the various atomistic mechanisms governed by different barriers freeze out or get activated at different temperatures, depending on their corresponding energy barriers.[38]

Comparison or extrapolation to other materials is possible if the energy-barrier set is similar to that of Pb(111). Then the Debye frequency sets the time scale while the energy barriers set the temperature scale, as one can readily deduce it from Eq. (15). On the other hand, if the energy-barrier set is completely different, as for example for Si,[39] it gives rise to a different rate-limiting mechanism namely attachment-detachment for a wide range of temperatures, and such extrapolation is not possible, but a whole set of simulations should be done for the group of materials with this type of barrier.

VI. CONCLUSIONS

In this paper we deduce energetic and kinetic parameters of a particular metal surface below its roughening temperature. We use kinetic Monte Carlo simulations to mimic the fluctuations of large nanoscale islands on these smooth surfaces in order to determine equilibrium island shapes, anisotropic line tensions in the azimuthal directions of the surface, and the correlation times of the Fourier modes of the fluctuations.

We derive an analytic expression for the chemical potential of the island edge from the equilibrium island shape and the associated capillary wave fluctuations around it. This chemical potential sets the scale for the anisotropic line tension (the azimuthal dependence of) which is usually known only up to a multiplicative constant. To account for the anisotropy of the line tension, this procedure contains a transformation from the Fourier modes of the island edge fluctuations to the true eigenmodes. However, detailed analysis of the Fourier and eigenmodes of the fluctuations reveals that the difference in their spectrum (Fig. 4) is unexpectedly small.

The obtained line tensions—one of the most important physical parameters of steps on surfaces—are in the correct range compared to known experimental results, even in this simplistic model, with its rather small set of hopping-energy barriers in the KMC simulation.

We have analyzed the effect of spatial sampling, which shows that the long wavelength modes are hardly affected by the undersampling (oversampling)—too low (too high) resolution of imaging, which means that there are fewer (more) sample points on the step edge in the image than actual atoms in the experiment—whereas moderately short and short modes change significantly.

The analyses of the correlation times of the Fourier modes show that nanoscale objects fluctuate on the ms to μs time range at moderately high temperatures (400 K) on Pb surfaces. Since the atomic processes are activated, this time scale changes dramatically with temperature.

In closing, we comment on the equilibration time of step structures in Monte Carlo simulations. The full equilibration of these structures is signalled by the correlation time of the longest wavelength mode, which can be very large (in CPU time) for the system sizes and temperatures studied in this paper. To do correct MC measurements in equilibrium, one must pass this time; otherwise, results for "equilibrium quantities" can be very misleading, as is well known from nonequilibrium statistical mechanics. If one does not look at correlation times of Fourier modes, very careful analysis is required to avoid such equilibration problems.[29] Recently, several papers have appeared concerning correlation functions, persistence, etc., of steps much longer than ours,[42] and sometimes even several of them (in studies of the interaction between them). They might well suffer from these problems since this equilibration time scales with system size as the fourth power, meaning that a system that is two times as big needs an order of magnitude longer CPU time to be equilibrated.

We also point out that the measurement of these fluctuations experimentally might be difficult because of the above-mentioned time scale of the fluctuations. One must either use techniques with which snapshots of the surface can be taken,[15] or, in direct visualization methods (like STM measurements), the scan rate of the equipment must be faster than the fluctuations of a given wavelength of interest. Otherwise one measures the two ends of a wavelength at such a time separation that they are uncorrelated, leading to difficulties of interpretation. The "speed" of the fluctuations can be tuned by changing the temperature, but one also must take into account that lowering the temperature decreases the size of the fluctuations, rendering the measurement harder.

Finally, the extrapolation of our results for nano-objects to mesoscale features makes possible comparisons of correlation times of modes of certain wavelengths, as well as of decay or of relaxation of larger structures to their equilibrium forms. This comparison reveals that the relaxation of 3D structures of the same lengths are slower than that of the simple step or monatomic high islands, due to additional mechanisms and phenomena like a possible Ehrlich-Schwoebel barrier, very low detachment rate and perhaps elasticity that affect the 3D structure.

*Corresponding author. Electronic address: szalmaf@physics.umd.edu

†Electronic address: einstein@umd.edu; URL: http://www2.physics.umd.edu/~einstein

[1] For a general introduction to crystal surface phenomena, see A. Pimpinelli and J. Villain, *Physics of Crystal Growth* (Cambridge University Press, Cambridge, 1998).

[2] For a review of vicinal surfaces, see H.-C. Jeong and E. D. Williams, Surf. Sci. Rep. **34**, 171 (1999).

[3] T. Müller and W. Selke, Eur. Phys. J. B **10**, 549 (1999).

[4] K. Morgenstern, E. Lægsgaard, and F. Besenbacher, Phys. Rev. B **66**, 115408 (2002).

[5] K. Thürmer, J. E. Reutt-Robey, E. D. Williams, M. Uwaha, A. Emundts, and H. P. Bonzel, Phys. Rev. Lett. **87**, 186102 (2001).

[6] G. Schulze Icking-Konert, M. Giesen, and H. Ibach, Phys. Rev. Lett. **83**, 3880 (1999).

[7] S. Dieluweit, H. Ibach, M. Giesen, and T. L. Einstein, Phys. Rev. B **67**, 121410 (2003).

[8] N. C. Bartelt, J. L. Goldberg, T. L. Einstein, E. D. Williams, J. C. Heyraud, and J.-J. Métois, Phys. Rev. B **48**, 15 453 (1993).

[9] S. Kodambaka, V. Petrova, S. V. Khare, D. Gall, A. Rockett, I. Petrov, and J. E. Greene Phys. Rev. Lett. **89**, 176102 (2002).

[10] S. Kodambaka, S. V. Khare, V. Petrova, D. D. Johnson, I. Petrov, and J. E. Greene, Phys. Rev. B **67**, 035409 (2003).

[11] S. V. Khare and T. L. Einstein, Phys. Rev. B **54**, 11 752 (1996).

[12] D. C. Schlößer, L. K. Verheij, G. Rosenfeld, and G. Comsa, Phys. Rev. Lett. **82**, 3843 (1999).

[13] S. V. Khare, S. Kodambaka, D. D. Johnson, I. Petrov, and J. E. Greene, Surf. Sci. **522**, 75 (2003).

[14] S. V. Khare and T. L. Einstein, Phys. Rev. B **57**, 4782 (1998).

[15] N. C. Bartelt and R. M. Tromp, Phys. Rev. B **54**, 11 731 (1996).

[16] A. L. Barabási and H. E. Stanley, *Fractal Concepts in Surface Growth* (Cambridge University Press, Cambridge, 1995).

[17] A. Pimpinelli, J. Villain, D. E. Wolf, J. J. Métois, J. C. Heyraud, I. Elkinani and G. Uimin, Surf. Sci. **295**, 143 (1993).

[18] G. S. Bales and A. Zangwill, Phys. Rev. B **41**, 5500 (1990).

[19] W. W. Mullins, J. Appl. Phys. **28**, 333 (1957); **30**, 77 (1959).

[20] W. W. Mullins, *Metal Surfaces: Structure, Energetics and Kinetics* (American Society of Metals, Metals Park, Ohio, 1963), p. 17.

[21] L. D. Landau and E. M. Lifshitz, *Statistical Physics*, Part I, 3rd ed. (Butterworth-Heinemann, Washington, DC, 1980), Chap. 15.

[22] S. Kodambaka, V. Petrova, S. V. Khare, D. D. Johnson, I. Petrov, and J. E. Greene, Phys. Rev. Lett. **88**, 146101 (2002).

[23] J. G. McLean, B. Krishnamachari, D. R. Peale, E. Chason, J. P. Sethna, and B. H. Cooper, Phys. Rev. B **55**, 1811 (1997).

[24] M. Zinke-Allmang, L. C. Feldman, and M. H. Grabow, Surf. Sci. Rep. **16**, 377 (1992).

[25] A. B. Bortz, H. M. Kalos, and J. L. Lebowitz, J. Comput. Phys. **17**, 10 (1975).

[26] M. E. J. Newman and G. T. Barkema, *Monte Carlo Methods in Statistical Physics* (Clarendon, Oxford, 1999).

[27] M. I. Haftel and M. Rosen, Phys. Rev. B **51**, 4426 (1995); Surf. Sci. **407**, 16 (1998).

[28] H. S. Lim, C. K. Ong, and F. Ercolessi, Surf. Sci. **269/270**, 1109 (1992); http://www.fisica.uniud.it/ ercolessi/potentials/Pb/

[29] F. Szalma, W. Selke, and S. Fischer, Physica A **294**, 313 (2001).

[30] A. Karim, M. Rusanen, I. T. Koponen, T. Ala-Nissila, and T. S. Rahman, Surf. Sci. **554**, L113 (2004).

[31] C. Bombis, A. Emundts, M. Novicki, and H. P. Bonzel, Surf. Sci. **511**, 83 (2002).

[32] N. C. Bartelt, J. L. Goldberg, T. L. Einstein, and E. D. Williams, Surf. Sci. **273**, 252 (1992).

[33] N. C. Bartelt, T. L. Einstein, and E. D. Williams, Surf. Sci. **312**, 411 (1994).

[34] B. Blagojević and P. M. Duxbury, Phys. Rev. E **60**, 1279 (1999).

[35] N. W. Ashcroft and N. D. Mermin, *Solid State Physics* (Saunders College, Philadelphia, 1976).

[36] L. Kuipers, M. S. Hoogeman, J. W. M. Frenken, and H. van Beijeren, Phys. Rev. B **52**, 11 387 (1995).

[37] S. Speller, W. Heiland, A. Biedermann, E. Platzgummer, C. Nagl, M. Schmid, and P. Varga, Surf. Sci. **331**, 1056 (1995).

[38] A. Bogicevic, J. Strömquist, and B. I. Lundqvist, Phys. Rev. Lett. **81**, 637 (1998).

[39] J. M. Bermond, J. J. Métois, X. Egéa, and F. Floret, Surf. Sci. **330**, 48 (1995).

[40] F. Szalma *et al.* (unpublished).

[41] D. B. Dougherty and F. Szalma (unpublished).

[42] For example, perhaps for large $\tilde{A}$; H. Gebremariam, S. D. Cohen, H. L. Richards, and T. L. Einstein, Phys. Rev. B **69**, 125404 (2004).